Egocentric Video Biometrics

Yedid Hoshen Shmuel Peleg
The Hebrew University of Jerusalem
Jerusaem, ISRAEL

Abstract

Egocentric cameras are being worn by an increasing number of users, among them many security forces worldwide. GoPro cameras already penetrated the mass market, and Google Glass may follow soon. As head-worn cameras do not capture the face and body of the wearer, it may seem that the anonymity of the wearer can be preserved even when the video is publicly distributed.

We show that motion features in egocentric video provide biometric information, and the identity of the user can be reliably determined from a few seconds of video captured when the user is walking. The proposed method achieves more than 90% identification accuracy in cases where the random success rate is only 3%.

Applications may include theft prevention of wearable cameras by locking the camera when not worn by its lawful owner. This work can also provide the first steps towards searching on video sharing services (e.g. YouTube) for egocentric videos shot by a specific person. An important message in this paper is that people should be aware that sharing egocentric video will compromise their anonymity, even when their face is not visible.

1. Introduction

The popularity of head worn Egocentric cameras is increasing. GoPro cameras are now used not only by extreme sports enthusiasts but also by law enforcement and military personnel. With the forthcoming release of Google Glass such cameras will further penetrate the mass market.

Special features of Egocentric video include:

- The camera is worn on the user, and is continuously recording while the user performs normal activities.
- The camera moves together with the user's head.
- The camera does not record images of the user. We show however that users can sometimes be identified.

As shown in social media (Fig. 1), users feel secure that sharing their egocentric videos does not compromise their identity. Police forces routinely release footage of officer activity, and commando operations recorded by cameras worn on soldiers heads are widely published on YouTube. Some have even recorded and published their own crimes. A consequence of our work is that the user identity of such videos can be found from camera motion in many cases.

It has previously been established that people can be distinctly identified by biometric characteristics such as height, stride length, walking speed, etc. Much research has been performed to extract and compare gait information from a video observing a walking person [10, 15, 4]. Unlike these methods, we identify the user from video recorded by a camera that he wears. The user is of course not visible in the video.

Gait analysis from non-visual devices such as accelerometers [19] and pressure-sensors [1] yields good performance on identification and verification tasks. Egocentric video can serve as a head mounted 2D visual gyroscope and can exploit similar information. Instead of requiring that users carry special-purpose measurement devices, we use gait information that is embedded in motion of the egocentric video published by the user.

Specifically we use sparse optical flow vectors (50 flow vectors per frame) taken over a few steps (4 seconds). This results in a set of time-series, one for each component of each optical flow vector. In Fig 2 we show the temporal Fourier Transform of one flow vector for three different sequences, showing visible differences between different people.

As a first approach for determining user identity, we computed LPC (Linear Predictive Coding [1]) [5] coefficients for each of the optical flow time series. All LPC coefficients of all optical flow sequences were used as a descriptor. Person identification using a non-linear SVM trained on the LPC descriptor gave 81% identification accuracy (vs. random 3%) and verification EER (Equal Error Rate) of 10%.

Our second approach learns the descriptor and classifiers using a Convolutional Neural Network (CNN) which

[1]The LPC coefficients of a time series are k values that when scalar multiplied with the last k measurements of the time series, will optimally predict the next measurement.

a) b) c)

Figure 1. a) A GoPro video uploaded to YouTube allegedly capturing a crime from the POV of the robber. Can the robber be identified? b) A GoPro video uploaded by US soldiers in combat. Are their identities safe? c) Combating theft of egocentric devices.

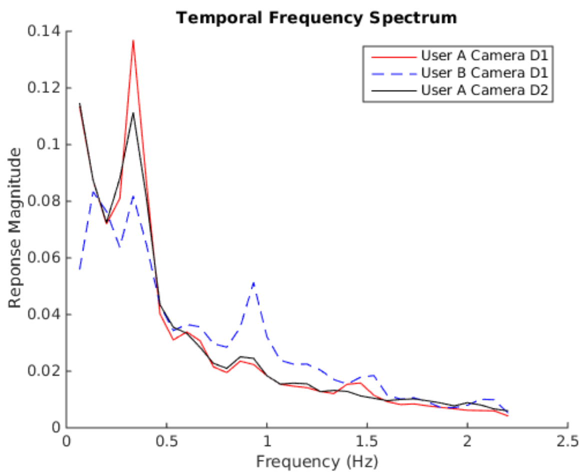

Figure 2. Comparison of the temporal frequency spectra for three videos. Two videos were recorded using camera D1 by users A and B, the third video was recorded by user A using camera D2. It is readily seen that the spectra of the two videos recorded by user A are very similar to each other despite being recorded by different cameras and at different times. This suggests that a person's physique is expressed in the motion observed in his video.

includes layers corresponding to gait descriptor extraction and to classification. The CNN is trained on the optical-flow features described above. Using CNN improves the results over the LPC coefficients, yielding 90% identification rate (vs. random 3%) and verification EER (Equal Error Rate) of 8%.

The above experiments were performed on both a small (6 person) public dataset [8] (originally collected for Egocentric Activity Analysis) and on a new, larger (32 person) dataset collected by us especially for Egocentric Video Biometrics.

The ability to determine the identity of the user quickly and accurately can be important for camera theft prevention and for forensic analysis (e.g. who committed the crime). Another application is web search for egocentric videos shot by a given person. Wearing a mask does not reduce recognition rate, of course.

2. Previous Work

Much work has been done on human biometrics. Some popular biometric measures are face recognition [29], speaker voice identification [3] and fingerprint recognition [18]. A review of biometric measures is presented in [11].

An important and longstanding biometric measure is Gait, an analysis of a person's walking style. A pioneering work by Murray [21] showed that gait is a highly distinctive biometric measure. Over the last few decades much work has been done on extracting gait information from videos obtained by static cameras ([10, 15, 4]). The spatial shape of the body is commonly used (e.g. [27]). This encodes measures such as height, width, leg length. Another popular class of features is temporal based features (e.g. [20]). Such information encodes information such as step velocity, acceleration and frequency. Several works studied gait analysis from non-visual sensors such as accelerometers [19] and pressure sensors [1].

Little work has been done on gait obtained from moving cameras. In a pioneering work, Shiraga et al. [26] have studied identifying persons from backpack mounted stereo cameras. By estimating rotation and period of motion using 3D geometry they were able to identify users with great accuracy. This however has the disadvantage of requiring specialized equipment. We instead learn gait features from widely used standard head-mounted cameras.

Using optical flow for activity recognition from head-mounted cameras has been done by [13, 23, 25, 16] and others. Poleg et al. [22] used optical flow vectors for hiding away the identity of the camera user. Yonateni et al [28] use head motion to retrieve head-mounted camera users observed in other videos recorded at the *same time*. We on the other hand use camera motion to identify users of wearable cameras *across time*.

Feature design for time series data has been extensively studied. It is particularly important for speech recognition systems ([24]). Speaker verification is a long standing problem which is related to this work. Linear Predictive Coding (LPC) [9]-based descriptors were found to be effective for speaker recognition. Here we show an LPC-based descriptor that is highly effective for user recognition from egocen-

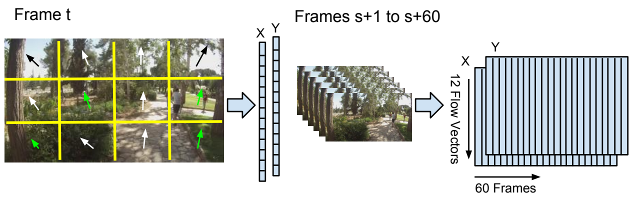

a) b)

Figure 3. a) 50 Optical flow vectors are calculated for each frame (only 12 shown here), and represented as two columns (each of 50 values), for the x and y optical flow components. b) The feature vector consists of optical flow columns for 60 frames, stacked into two 50×60 arrays, for the x and y components of the flow.

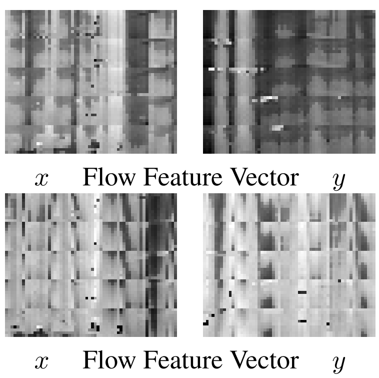

Figure 4. Two examples of the flow feature vectors. Each feature vector consists of 50 optical flow vectors per frame (shown in vertical axis), computed for each of 60 frames (the horizontal axis). The left and right images show the x and y components of the optical flow.

tric camera video.

Another approach is learning features along with the classifier end-to-end, instead of hand designing them. We perform this using convolutional neural networks (CNN). For an overview of deep networks see [2]. Learned features are sometimes better than hand-designed features [14].

3. Identifying Users using Optical Flow

Egocentric video suffers from bouncy and unsteady motion caused by user head and body motion. Although usually a nuisance, we show that this motion forms the basis for accurate person identification methods.

We present our basic features in Sec. 3.1. Two alternative descriptors and classifiers are described in Sec. 3.2 and Sec. 3.3.

3.1. Feature Extraction

In the following sections we assume that the video frames were preprocessed in the following way (see Fig. 3):

1. Frames are partitioned into a small number ($m_x \times m_y$) of non-overlapping blocks.
2. $m_x \times m_y$ optical flow vectors are computed for each frame using the Lucas Kanade algorithm [17]. We use 10×5 optical flow vectors per frame.
3. A block of T seconds of such optical flow vectors is taken. We used $T = 4$ seconds, which is long enough to include a few steps. At 15 fps this results in 60 frames.
4. Each feature vector covers a period of 4 seconds, and we computed feature vectors every 2 seconds. There is an overlap of 2 seconds between two successive feature vectors.

We used optical flow features for user identification, rather than pixel intensities, as the gait is eventually expressed by the pixel motion. On the other hand, user identification should be invariant to the specific objects seen in the environment, objects that are represented by pixel intensities. CNNs may be able to learn optical flow from pixel intensities, but learning this will require much more data than we can collect.

If dense optical flow were used as a feature, the high feature dimensionality would have lead to overfitting on small datasets. In looking for the optimal feature size we found out that a grid size of 10×5 optical flow vectors was a good compromise between overfitting and accuracy. Using a smaller number of flow vectors gave reduced accuracy.

The feature extraction process is shown in Fig 3. Visualization of two extracted feature vectors is shown in Fig. 4. Full details are in Sec. 6.3.

3.2. LPC Descriptor + Kernel SVM

LPC [5] is a popular time-series descriptor (e.g. for speaker verification). LPC assumes the data is generated by a physical system, here the person's head and body. It attempts to learn a linear regression model for its equations of motion, predicting for each optical flow series the flow value in the next frame given the flow values of previous k frames. Given a feature vector, we calculate an LPC model for each component of each 4s flow time series (100 models in total). Using too few coefficients yields less accurate predictions, while too many coefficients causes overfitting. We found $k = 9$ to work well for our case. The final LPC descriptor consisted of all coefficients of all time-series models (100×9).

An RBF-SVM classifier was used for learning both identification (classify LPC descriptor into 1 of M known people) and verification (classify LPC descriptor into target person or non-target person). The non-linear (RBF) classifier was found to out-perform linear SVM in almost all cases. As mentioned before, person identification using a non-linear SVM trained on the LPC descriptor gave 81% identification rate (vs. random 3%), and verification EER (Equal Error Rate) was 10%.

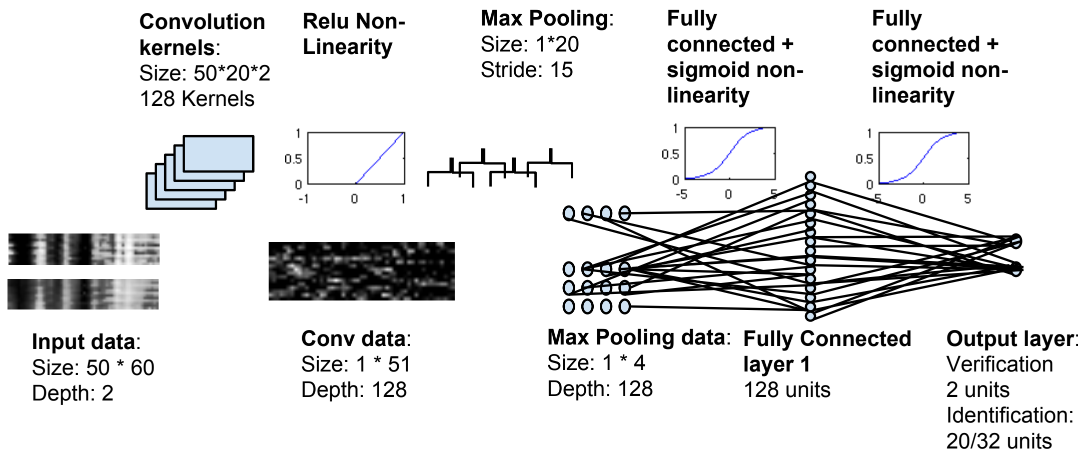

Figure 5. A diagram of our CNN architecture for user recognition from a given flow feature vector. The operations on the data are shown on top, the sizes of subsequent data layers are shown on the bottom. The Neural Network learns the descriptor jointly with the classifier, therefore automatically creating a descriptor optimal to this task.

3.3. Convolutional Neural Network

In Sec. 3.2 we described a hand-designed descriptor for identity classification. The LPC descriptor suffers from several drawbacks:

- The LPC regression model is learned for each time-series separately and ignores the dependence between optical flow vectors.
- The LPC descriptor and SVM classifier are learned independently, the labels cannot directly influence the design of the descriptor.

To overcome the above drawbacks, we propose to learn a CNN model for identity recognition. The CNN learns descriptor and classifier end to end, and is able to take advantage both of dataset labels and the dependence between features when calculating filter coefficients. The CNN is more general architecture, the LPC descriptor is a subset of descriptors learnable by the network.

Due to the limited number of data points available in our datasets, we limit our CNN to only 2 hidden layers. Using more layers increases model capacity but also increases over-fitting. The architecture is illustrated in Fig. 5.

Our architecture is tailored especially for egocentric video. As we use sparse optical flow we do not assume much spatial invariance in the features (differently from most image recognition tasks). On the other hand the precise temporal offset of the user's actions is usually not important, e.g. the precise time of the beginning of a user's step is less important than the time between strides. Our architecture should therefore be temporally invariant. The first layer was thus designed to be convolutional in time but not in space.

The kernel size spans all the blocks across the x and y components over K_T frames (we use $K_T = 20$ which is a little longer than the typical step duration). The convolutional layer consists of M kernels (we use $M = 128$). The outputs of the kernels $z^1_m = W_m * x$ are passed through a ReLU non-linearity ($max(z^1_m, 0)$). We pool the outputs substantially in time, as the feature vector is of high dimension compared to the amount of training data available. To correspond to the typical time interval between steps we use kernel length of 20 and stride of 15.

The data is then passed through two fully connected (affine) layers each followed by a sigmoid non-linearity ($\sigma(z) = \frac{1}{1+e^{-z}}$). The first fully connected hidden layer has N_1 hidden nodes (we used $N_1 = 128$). The output of this layer is the learned CNN descriptor.

The second fully connected layer is a linear soft-max classifier and has the same number of nodes as the number of output classes: 2 classes for the verification case, and 20-32 classes in the identification cases.

3.4. Joint Prediction from Several Descriptors

Sec. 3.2 and Sec. 3.3 described a method to train an identity classifier on a short (4 seconds) video sequence. The video used for classification is usually significantly longer than 4 seconds.

We split the video into 4 second subsequences and classify each using LPC or CNN classifiers, We then classify the video into the globally most likely label, $argmax_i \prod_t P(L_t = i|V_t) = argmax_i \sum_t log(P(L_t = i|V_t))$. While this classifier assumes that feature vectors are IID, we have found that this requirement is not necessary for the success of the method. See Fig. 6 for an example on the FPIS dataset.

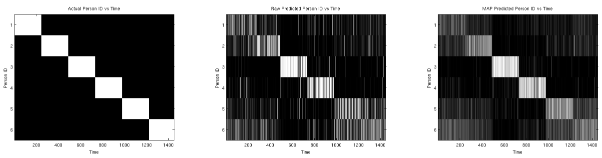

a) b) c)

Figure 6. The MAP rule operated on the FPIS dataset: a) Ground truth labels. b) Raw CNN probabilities. c) MAP rule probabilities (for $T = 12$ seconds.). The MAP classifier visibly 'cleaned up' the prediction.

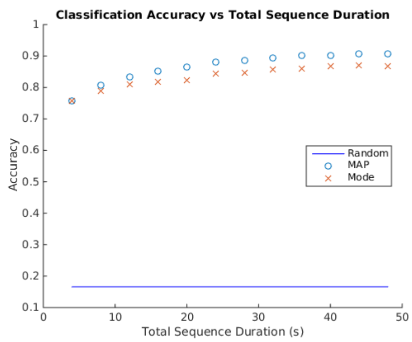

Figure 7. Classification accuracy vs. video length when one feature vector covers $T = 4$ seconds (Using CNN on the FPSI Dataset). Longer video allows extraction of more feature vectors. MAP classification consistently beats mode classification. Both methods can exploit longer sequences and thus improve on 4s sequence identification. All methods perform far better than random.

MAP classification has helped boost the identification performance on the EVB dataset to around 90% (an increase of 13%) over the 4s rate.

4. Results

Several experiments were performed to verify the effectiveness of our method. As there is no standard dataset for Egocentric Video Biometrics, we use both a small (6 person) public dataset - FPSI [8] that was originally collected for egocentric activity analysis. For each user - morning sequences were used for training, and afternoon sequences for testing.

In order to evaluate our method under more principled settings, we collected a new larger (32 person) dataset - EVB - specifically designed for egocentric user recognition. In the EVB dataset all users recorded two 7 minute sequences (from which we extracted around 200 four second sequences each) on the same day with different head-mounted cameras (D1,D2) for training and testing. 20 of the users also recorded another 7 minute sequence with yet another camera (D3) a week later. Both datasets are described in detail in Sec. 6.1. The detailed experimental protocol is described in Sec. 6.2.

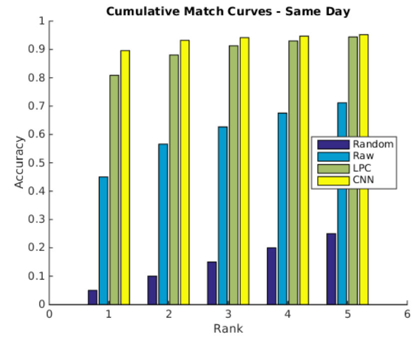

Figure 8. CMC rates for same day identification (for 12s sequences). LPC accuracy: 81% (Top-1) and 88% (Top-2). The CNN further improves the performance with 90% (Top-1) and 93% (Top-2). Both methods far outperform the random rate of 3% (Top-1) and 6% (Top-2). Both descriptors also beat the raw features by a large margin.

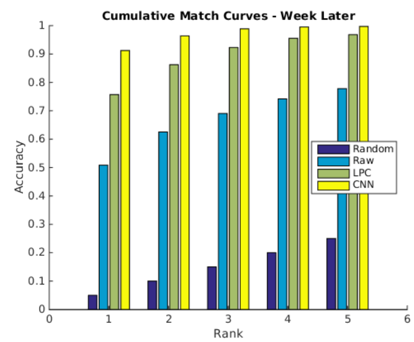

Figure 9. CMC rates for identification 1 week later (for 12s sequences). LPC accuracy: 76% (Top-1) and 86% (Top-2). The CNN further improves the performance with 91% (Top-1) and 96% (Top-2). Both methods far outperform the random rate of 5% (Top-1) and 10% (Top-2). Both descriptors also beat the raw features by a large margin.

4.1. Identification

Fig. 7 presents the person classification test performance of our network on the FPSI database (6 people). The average correct classification rate on a single feature vector (describing only 4 seconds of video) is 76% against the random performance of 16.6%.

Usually test videos are longer than 4 seconds, and we have multiple feature vectors for each person. We combine predictions over a longer video using the MAP rule in Sec. 3.4. In Fig. 7 we compare the MAP strategy vs. taking the most frequent 4s prediction in the test video (Mode). We observe that using longer sequences further improves the identification performance, reaching around 91% accuracy for 50 seconds of video. We can also observe that MAP classifiers consistently beats the Mode classifier and use it in all other experiments.

To evaluate the classification performance on a larger

Descriptor	No Stab 4s	No Stab 12s	Stab 4s	Stab 12s
LPC	65%	81%	59%	72%
CNN	77%	90%	71%	86%

Table 1. Same-day identification accuracy with and without stabilization.

dataset, we show the performance of our method on our new dataset - EVB. In this experiment the network was trained on video sequences for each person using Camera D1 and is evaluated on video sequences recorded on the same day using Camera D2 and a week later recorded using Camera D3. In Fig. 8 and Fig. 9 we present the cumulative match curve (CMC) for the same day and week later identification results respectively. We use the $Top\ k$ notion, indicating that the correct result appeared within the top k predictions of the classifier. In addition to LPC and CNN, an RBF-SVM trained on the raw optical flow features is used as baseline to evaluate the quality of our descriptors. High accuracy was achieved in both scenarios, same day CNN identification accuracy is 90% (top 1) and 93% (top 2). The identification performance a week later is better with 91% (top 1) and 96% (top 2). The improved performance numbers a week later are expected due to the smaller dataset size (20 vs 32), but are nonetheless encouraging as many participants wore different shoes from the D1 training sequence recorded a week before. This result shows that our method can obtain good identification performance on meaningful numbers of people and across at least a week.

To test the possibility that stabilization would take away some or all the gait information in the frame motions, the identification experiments were redone with the following pre-processing stage: for each frame (50 flow vectors) the mean framewise vector was calculated and then subtracted from each of the vectors in the frame. As motion between frames is small and some lens distortion correction was performed, this is similar to 2D stabilization. Table. 1 shows that such "stabilization" degrades performance somewhat (4-9%), but accuracy still remains fairly high. We note however that more complex stabilization might remove more gait information. This investigation is left for future work.

4.2. Verification

We also test the verification performance obtained by our method. In order to evaluate verification performance by a single number it is common to use the Equal Error Rate (EER), the error rate at which the False Acceptance Rate (FAR) and False Rejection Rate are equal.

The EER for both the CNN and LPC descriptors for videos of length 4s (one feature vector) and 12s (five feature vectors) is presented in Table. 2 while the ROC curves are shown in Fig. 10. A detailed description of our protocol can be found in Sec. 6. It can be seen from our results that high

Descriptor	4s	12s
LPC	13.6%	9.6%
CNN	11.3%	8.1%

Table 2. Verification equal error rates for LPC and CNN descriptors with 4s and 12s sequence duration.

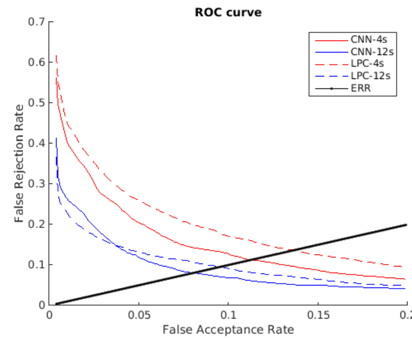

Figure 10. ROC curves for the verification performance of our method for LPC and CNN descriptors for 4s and 12s. High accuracy is obtained by both methods, CNNs outperformed LPCs particularly on short sequences. The EER of each method is given by the point of intersection between the linear line and its ROC curve.

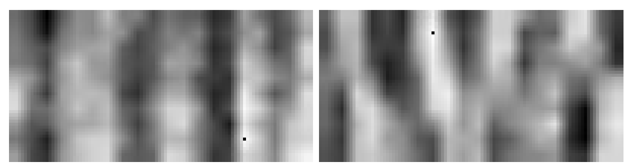

Figure 11. Examples of a temporal filter for the x and y flow components. Horizontal axis is time, and vertical axis is location along the central line. The x component filter appears to be sensitive for certain frequencies while the y component filter is sensitive to rotations.

verification rates can be obtained by both descriptors: LPC 14% (4s), 10% (12s) and CNN 11% (4s), 8% (12s). The CNN obtains better performance for both durations with a larger improvement for 4s.

It should be noted that all test probe persons apart from the target user had never been used in training. By modeling the target user we can separate him from the global population. Our results show our method is effective at learning the target person rather than attempting to model the general population, and is therefore able to generalize to unseen test users.

5. Discussion

Analysis of CNN features: In order to analyze the features learned by the CNN we visualize the filters learned by the first layer. Fig. 11 shows the x and y components of a first layer temporal filter learned by the network. For illustration purposes, only the weights of the central line of

a) b) c)

Figure 12. Common failure cases for the 4-second descriptor: a-b) Sharp turns of the head result in atypical fast motions, sometimes causing motion blur. c) Large moving objects can also cause atypical optical flow patterns.

pixels are shown. Looking at the weights, we see that the x component filter is tuned to respond to some specific frequencies, while the y component looks for sharp rotations. This behavior appears in several other filters suggesting that the network might be using both spectral and transitive cues.

Transfer Learning for Verification: In some scenarios it may not be possible to train a verification classifier for each person. In such cases Nearest Neighbors may be a good alternative. The following approach is taken: An identification CNN is trained on half the people in the training dataset. We choose a video by a target person (that was not used for training the CNN), and extract its CNN descriptors (as in Sec. 3.3), this set of descriptors forms our gallery. Similarly we extract CNN descriptors from all video sequences of persons not used for training the CNN, this forms our probe set (excluding the sequence used as gallery). For each probe descriptor we check if the euclidean distance from its nearest neighbor in the gallery is smaller than some threshold, and if so we classify it as the target person. We used Camera D1 sequences for training and D2 sequences for test. 16 randomly selected people were used for training the CNN, and the rest for verification. The same procedure was carried out for LPC (without training a CNN). Multiple 4s sequence predictions are aggregated using simple voting. The average EER for 12s sequences was 15.5% (CNN) and 22%(LPC). Although less accurate than trained verification, this shows the network learns identity features that are general and can be transferred to identify unseen people. Nearest Neighbors on the optical flow raw features yielded very low performance in accordance with the findings of [22, 28].

Verification on FPSI: We tried learning a verification classifier by choosing one person from the FPSI dataset as target, and 4 other users as negative training data. The morning sequences of the target person were used for training and the afternoon for testing. We tested the verification performance between the afternoon sequences of the target user and the remaining 6th non-target user from the FPSI dataset. The network however, fit to the train non-target users and has not been able to generalize to the unseen probe user. We therefore conclude that a significant number of users (such as present in the EVB dataset) is required for training a verification classifier.

Failure cases: In Fig. 12 several cases are shown where the 4 second descriptor failed to give correct identification. Failure can be caused by sharp head movements (sometimes causing significant blur), by large moving objects, or by lack of features for optical flow computation. It is likely that by identifying such cases and removing their descriptors, higher recognition performance may be achieved.

6. Experimental Procedure

In this section we give a detailed description of the experimental procedure used in Sec. 4.

6.1. Dataset Description

Two datasets were used for evaluation: a public general purpose dataset (FPSI) and a larger dataset (EVB) collected by us to overcome some of the weaknesses of FPSI.

6.1.1 FPSI Dataset

The First-Person Social Interactions (FPSI) dataset was collected by Fathi et al. [8] for the purpose of activity analysis. 6 individuals (5 males, 1 female) recorded a day's worth of egocentric video each using head-worn GoPro cameras. Due to battery and memory limitations of the camera, the users occasionally took the cameras off and put them on again, ensuring that camera extrinsic parameters were not kept constant.

In this work we learn human biometrics while walking, rather than sitting or standing. We therefore extracted the walking portions of each video using manual labels. It is possible to use a classifier such as described in [23] to find the walking intervals.

6.1.2 EVB Dataset

The FPSI dataset suffers from several drawbacks: it contains video only for a small number of users (6) and each participant wears the same hat and camera all the time. It is therefore conceivable that learning camera parameters can help identification. To overcome these issues we collected a larger dataset - Egocentric Video Biometrics (EVB).

The EVB consists of head-mounted video sequences collected from 32 participants. Each video sequence was recorded with a GoPro camera attached to a baseball cap worn on the participant's head (as in Fig. 13). Each participant was asked to walk normally for around 7 minutes along the same road. All participants recorded two 7 minute video sequences on a single day using two different cameras (and caps). 20 participants also recorded another sequence a week later. The use of different cameras for different sequences came to ensure that motion rather than camera calibration is learned. No effort was made to ensure that the

Figure 13. The apparatus used to record the EVB dataset.

same shoes would be used on both days (and in fact several persons had changed shoes between sequences).

6.2. Evaluation Protocol

6.2.1 User Identification

User identification sets to identify a user from a closed set of M people. For this task it is assumed that we have training data from all users.

We tested our method both on the FPSI the EVB datasets. In the FPSI dataset we used for each individual the first 80% of sequences (taken in the morning) for training, and the last 20% sequences recorded in the afternoon for testing. This is done to reduce overfitting to a particular time or camera setup. Data were randomly sub-sampled to ensure equal number of examples for each person in both training and testing sets. The results are described in Sec. 4.

For the EVB dataset we used sequences from Camera D1 for training. For testing we use both sequences from Camera D2 (taken on the same day) and Camera D3 (taken a week later, when available). The results on each camera are compared to analyze whether identification performance degrades within a week.

6.2.2 User Verification

Given a target user with a few minutes of training data, and negative training examples by other non-target users, we verify whether a probe test video sequence was recorded by the target user. Verification on longer sequences is done by combining the predictions from subsequent short sequences. As the FPSI dataset contains only 6 users it was not suitable for the verification task (this was elaborated upon in Sec. 5) therefore only the EVB dataset was used for evaluating performance on this task. For each of 32 participants: i) participant is designated target user ii) we selected sequences of the target user and 15 non-target users (randomly selected) for training a binary classifier. All training sequences were 7 minutes (200 descriptors) long and were recorded by camera D1. iii) Another sequence recorded by the target user and the remaining 16 participants that were not used for training, were used to test the verification classifier. Test sequences were recorded by camera D2. iv) The ROC curve and EER ware computed. Average EER and ROC for all participants is finally obtained. As each sequence contained about 200 descriptors this formed a significant test set. Care was taken to ensure that all users (apart from the target user) would appear in the training or test datasets but not in both. This was done to ensure we did not overfit to specific non-target users. We replicated positive training examples to ensure equal numbers of negative and positive training and test data.

6.3. Implementation Details

Features: In all experiments the optical flow grid size used was 10×5. In the CNN experiments, all optical flow values were divided by the square-root of their absolute value, this was found to help performance by decreasing the significance of extreme values. Feature vectors of length 60 frames at 15 fps (4s) were used. Feature vectors were exatracted every 2s (with a 2s overlap).

Normalization: We followed the standard practice - For the LPC descriptor, all feature vectors were mean and variance normalized across the training set before being used by the SVM. For the CNN, feature vectors were mean subtracted before being input to the CNN.

Training: The SVM was trained using LIBSVM [6]. We used $\sigma = 1e-4$ and $C = 1$ for LPC, $C = 10$ for the raw features. The CNN was trained by AdaGrad [7] with learning rate 0.01 on a GPU using the Caffe [12] package. The mini-batch size was 200.

7. Conclusion

A method to determine the identity of a user from head-worn egocentric camera video has been presented. We show that user identity can be found from gait information as expressed in camera motion when walking. Recognition was done with both physically motivated hand designed descriptors, and with a Convolutional Neural Network. Both methods gave good performance for identification and for verification. The CNN classifier was shown to generalize and improve on the LPC hand-designed descriptor.

The time-invariant CNN architecture presented here is quite general and can be used for other video classification tasks relying on coarse optical flow.

We have tested the effects of simple 2D video stabilization on classification accuracy, and found only slight degradation in performance. It is possible that more elaborate stabilization would have a greater effect.

The implication of our work is that users' head-worn egocentric videos give much information away. This information can be used benevolently (e.g. camera theft prevention, user analytics on video sharing websites) or maliciously. Care should therefore be taken when sharing such video.

Acknowledgement: This research was supported by Israel Science Foundation.

References

[1] S. J. M. Bamberg, A. Y. Benbasat, D. M. Scarborough, D. E. Krebs, and J. A. Paradiso. Gait analysis using a shoe-integrated wireless sensor system. *IEEE Trans. on Information Technology in Biomedicine*, 12(4):413–423, 2008. 1, 2

[2] Y. Bengio. Learning deep architectures for ai. *Foundations and trends in Machine Learning*, 2(1):1–127, 2009. 3

[3] F. Bimbot, J.-F. Bonastre, C. Fredouille, G. Gravier, I. Magrin-Chagnolleau, S. Meignier, T. Merlin, J. Ortega-García, D. Petrovska-Delacrétaz, and D. A. Reynolds. A tutorial on text-independent speaker verification. *EURASIP*, 2004:430–451, 2004. 2

[4] A. F. Bobick and A. Y. Johnson. Gait recognition using static, activity-specific parameters. In *CVPR*, 2001. 1, 2

[5] J. P. Campbell Jr. Speaker recognition: a tutorial. *Proceedings of the IEEE*, 85(9):1437–1462, 1997. 1, 3

[6] C.-C. Chang and C.-J. Lin. LIBSVM: A library for support vector machines. *ACM Trans. on Intelligent Systems and Technology*, 2011. 8

[7] J. Duchi, E. Hazan, and Y. Singer. Adaptive subgradient methods for online learning and stochastic optimization. *JMLR*, 2011. 8

[8] A. Fathi, J. K. Hodgins, and J. M. Rehg. Social interactions: A first-person perspective. In *CVPR*, 2012. 2, 5, 7

[9] S. Furui. Cepstral analysis technique for automatic speaker verification. *ICASSP*, 1981. 2

[10] J. Han and B. Bhanu. Individual recognition using gait energy image. *IEEE Trans. PAMI*, 2006. 1, 2

[11] A. K. Jain, P. Flynn, and A. A. Ross. *Handbook of biometrics*. Springer, 2007. 2

[12] Y. Jia, E. Shelhamer, J. Donahue, S. Karayev, J. Long, R. Girshick, S. Guadarrama, and T. Darrell. Caffe: Convolutional architecture for fast feature embedding. *arXiv preprint arXiv:1408.5093*, 2014. 8

[13] K. M. Kitani, T. Okabe, Y. Sato, and A. Sugimoto. Fast unsupervised ego-action learning for first-person sports videos. In *CVPR*, 2011. 2

[14] A. Krizhevsky, I. Sutskever, and G. E. Hinton. Imagenet classification with deep convolutional neural networks. In *NIPS*, 2012. 3

[15] L. Lee and W. E. L. Grimson. Gait analysis for recognition and classification. In *Automatic Face and Gesture Recognition*, 2002. 1, 2

[16] Z. Lu and K. Grauman. Story-driven summarization for egocentric video. In *CVPR*, 2013. 2

[17] B. D. Lucas, T. Kanade, et al. An iterative image registration technique with an application to stereo vision. In *IJCAI*, volume 81, pages 674–679, 1981. 3

[18] D. Maltoni, D. Maio, A. K. Jain, and S. Prabhakar. *Handbook of fingerprint recognition*. springer, 2009. 2

[19] J. Mantyjarvi, M. Lindholm, E. Vildjiounaite, S.-M. Makela, and H. Ailisto. Identifying users of portable devices from gait pattern with accelerometers. In *ICASSP*, 2005. 1, 2

[20] H. Murase and R. Sakai. Moving object recognition in eigenspace representation: gait analysis and lip reading. *PRL*, 17(2):155–162, 1996. 2

[21] M. P. Murray. Gait as a total pattern of movement: Including a bibliography on gait. *American Journal of Physical Medicine & Rehabilitation*, 46(1):290–333, 1967. 2

[22] Y. Poleg, C. Arora, and S. Peleg. Head motion signatures from egocentric videos. In *ACCV*, 2014. 2, 7

[23] Y. Poleg, C. Arora, and S. Peleg. Temporal segmentation of egocentric videos. In *CVPR*, 2014. 2, 7

[24] D. A. Reynolds and R. C. Rose. Robust text-independent speaker identification using gaussian mixture speaker models. *IEEE Trans. on Speech and Audio Processing*, 3(1):72–83, 1995. 2

[25] M. S. Ryoo and L. Matthies. First-person activity recognition: What are they doing to me? In *CVPR*, 2013. 2

[26] K. Shiraga, N. T. Trung, I. Mitsugami, Y. Mukaigawa, and Y. Yagi. Gait-based person authentication by wearable cameras. In *INSS*, 2012. 2

[27] L. Wang, T. Tan, H. Ning, and W. Hu. Silhouette analysis-based gait recognition for human identification. *IEEE TRans. PAMI*, 25(12), 2003. 2

[28] R. Yonetani, K. M. Kitani, and Y. Sato. Ego-surfing first person videos. In *CVPR*, 2015. 2, 7

[29] W. Zhao, R. Chellappa, P. J. Phillips, and A. Rosenfeld. Face recognition: A literature survey. *ACM Computing Surveys*, 35(4):399–458, 2003. 2